

Structure and Activity Analysis of Inauhzin Analogs as Novel Antitumor Compounds That Induce p53 and Inhibit Cell Growth

Qi Zhang^{1,2,3}, Derong Ding^{2,3}, Shelya X. Zeng^{1,2}, Qi-Zhuang Ye^{2*}, Hua Lu^{1,2,3*}

1 Department of Biochemistry and Molecular Biology and Tulane Cancer Center, Tulane University School of Medicine, New Orleans, Louisiana, United States of America, **2** Department of Biochemistry and Molecular Biology, Indiana University School of Medicine, Indianapolis, Indiana, United States of America, **3** Simon Cancer Center, Indianapolis, Indiana, United States of America

Abstract

Identifying effective small molecules that specifically target the p53 pathway in cancer has been an exciting, though challenging, approach for the development of anti-cancer therapy. We recently identified Inauhzin (INZ) as a novel p53 activator, selectively and efficiently suppressing tumor growth without displaying genotoxicity and with little toxicity to normal cells. In order to reveal the structural features essential for anti-cancer activity of this small molecule, we have synthesized a panel of INZ analogs and evaluated their ability to induce cellular p53 and to inhibit cell growth in cell-based assays. This study as described here leads to the discovery of INZ analog **37** that displays much better potency than INZ in both of p53 activation and cell growth inhibition in several human cancer cell lines including H460 and HCT116^{+/+} cells. This INZ analog exhibited much less effect on p53-null H1299 cells and HCT116^{-/-} cells, and importantly no toxicity on normal human p53-containing WI-38 cells. Hence, our results not only unveil key chemical features for INZ activity, but also identify the newly synthesized INZ analog **37** as a better small molecule for further development of anti-cancer therapy.

Citation: Zhang Q, Ding D, Zeng SX, Ye Q-Z, Lu H (2012) Structure and Activity Analysis of Inauhzin Analogs as Novel Antitumor Compounds That Induce p53 and Inhibit Cell Growth. PLoS ONE 7(10): e46294. doi:10.1371/journal.pone.0046294

Editor: Hirofumi Arakawa, National Cancer Center Research Institute, Japan

Received: June 5, 2012; **Accepted:** August 29, 2012; **Published:** October 24, 2012

Copyright: © 2012 Zhang et al. This is an open-access article distributed under the terms of the Creative Commons Attribution License, which permits unrestricted use, distribution, and reproduction in any medium, provided the original author and source are credited.

Funding: H.L. was supported by National Institutes of Health-National Cancer Institute grants CA127724, CA095441, CA172468, and CA129828. Q.-Z.Y. was supported by National Institute of Health grant AI065898.

Competing Interests: The authors have read the journal's policy and have the following conflicts: The authors are submitting a Patent application (pending) for the compounds as revealed in their manuscript through Indiana University, to which the authors are affiliated and which the authors may benefit from. This does not alter the authors' adherence to all the PLOS ONE policies on sharing data and materials.

* E-mail: hlu2@tulane.edu (HL); yeq@iupui.edu (Q-ZY)

These authors contributed equally to this work.

Introduction

The p53 tumor suppressor protein can prevent the formation of tumors through several mechanisms, including the activation of cell-cycle checkpoints to prevent damaged cells from proliferation (cell-cycle arrest and DNA repair), the promotion of senescence (permanent cell-cycle arrest), and/or the triggering of cell death (apoptosis or autophagy) [1,2]. It can also impede cell migration, metabolism, or angiogenesis, which are needed for cancer cell progression and metastasis [1]. Mutations of the tumor suppressor gene *TP53* are detected in ~50% of all types of human cancers [3], while the functions and stability of the p53 protein are often abrogated via posttranslational mechanisms in the rest of human cancers that contain wild type *TP53* [4,5]. Therefore, the restoration or reactivation of wild-type p53 function can lead to rapid elimination of tumors. As such, compounds that target the p53 pathway have become promising anticancer drug candidates, and several of them have entered clinical trials [4,6]. For instance, Nutlin-3 and MI-219 can increase p53 level and activity by interfering with the p53-MDM2 binding [7–9]. Even though there have been extensive endeavors to find small molecules that target the p53 pathway, none has yet proven to be clinically effective therapeutics due to the inherent undesirable toxicity to normal cells and tissues.

Through our recent efforts in conducting *in silico* screening and cellular-based assays [10], we discovered Inauhzin (INZ) and its analogs (**Figure 1**) as a novel class of small molecules that effectively activate p53 and promote p53-dependent apoptosis of human cancer cells without causing apparently genotoxic stress. In addition, INZ stabilized p53 by increasing p53 acetylation and preventing MDM2-mediated ubiquitylation of p53 in cells. Remarkably, INZ inhibited cell proliferation, induced senescence and tumor-specific apoptosis, and repressed the growth of xenograft tumors derived from p53-harboring lung cancer H460 and colon cancer HCT116^{+/+} cells without causing apparent toxicity to normal tissues.

INZ is an effective anti-cancer agent either alone or in combination with Nutlin treatment [11] or DNA damage agents Cisplatin and Doxorubicin (unpublished). Single treatment with Nutlin-3 is less efficient in inhibiting the growth or promoting apoptosis of some cancer cells, such as HCT116^{+/+}, H460, or A549, in xenograft tumor models even though these cells contain wild type p53. Combination of INZ with Nutlin-3 synergistically promotes apoptosis in HCT116^{+/+} and H460 cell lines in a p53-dependent fashion. This combination also synergistically activates p53 in xenograft tumors derived from these cancer cells and significantly suppresses their growth.

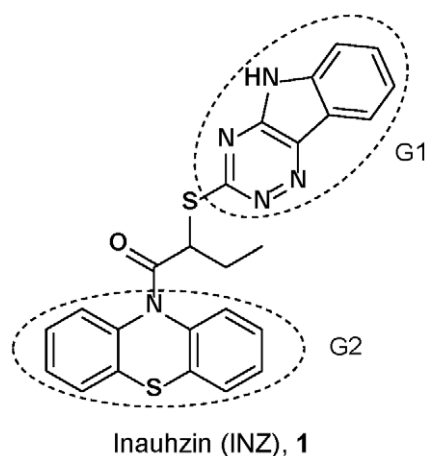


Figure 1. Structure of Inauhzin (INZ).
doi:10.1371/journal.pone.0046294.g001

To further characterize the structural features essential for the activity of this group of small molecules to induce p53 and to suppress cell proliferation, we initiated structure-activity relationship (SAR) analyses of INZ analogs. To this purpose, we synthesized a number of new INZ analogs and also evaluated their capability of p53 induction and cell growth inhibition using cell-based assays. Our study not only reveals critical chemical groups for INZ activity, but also leads to the discovery of INZ derivative **37** that displays better potency in p53 induction and cancer cell growth inhibition than does INZ.

Results and Discussion

Design and Chemical Synthesis

Within its structure, INZ (**1**) possesses two distinct chemical components: triazino[5,6-b]indole (G1) and phenothiazine (G2) moiety (Figure 1). In our preliminary SAR studies [10], we purchased 46 compounds analogous to INZ with diversities of G1 and G2 and investigated the activity of the compounds in cell-based assays for their ability to induce p53 levels in p53 containing human colon cancer HCT116^{+/+} cells and/or human lung cancer H460 cells using immunoblotting (IB) (Figure 2 and Figure 3). The results indicated that a unique structure scaffold might be required for the activity of INZ in cells. Removal of the ethyl group at R₁ (**S1–S3**) or modification at both R₂ and R₃ positions on the indole moiety of INZ (**S4**) disabled the compound's ability to activate p53 in cells (Figure 2). The R₂ position can be modified and substituted without loss of activity by replacing it with some alkyl groups, such as methyl, ethyl and allyl, but not propyl (**S5–S8**). Both triazino[5,6-b]indole (G1) and phenothiazine (G2) are essential functional groups for p53 induction. The analogs containing ethyl group at the R₁ position but lacking either functional groups G1 (**S9–S10**), or G2 (**S19–S22**) failed to induce p53. Compounds **S11–S18**, **S23–S28**, and **S29–S34** with different aromatic moieties other than triazino[5,6-b]indole at G1 and/or phenothiazine at G2 had very low or no activity. Overall, the results suggest that a specific chemical structure with the intact triazino[5,6-b]indole-3-ylthio]butanoyl]-10H-phenothiazine might be crucial for p53 activation in cells. Indeed, INZ (**1**) displayed more potent p53 activation and anticancer inhibition than either of its component fragments, compound **2'** or **3'** (Figure 4, and data not shown). It suggests that a synergism is achieved when these two structural units are combined within a single molecule. Therefore, we focused our attention on the structural modifica-

tions on the pharmacologically active core: triazino[5,6-b]indole or phenothiazine. Modifications included extension of carbon chain length on R₁ (**14**) (Figure 5), the substitution on the phenothiazine ring (G2) (**6–13**) (Figure 5) or on the triazino[5,6-b]indole ring (G1) (**15–36**) (Figure 5).

The syntheses of these new INZ derivatives are outlined in Figures 4, 6, 7, and 8.

The synthesis of compounds INZ (**1**) and **6–19** was outlined as Figure 6. The 5*H*-[1, 2, 4] triazino[5,6-*b*]indole-3-thiol **3** was prepared from the commercial isatin according to the standard procedure [12]. The bromide **5** was synthesized through refluxed thiophenol with the bromobutyl bromide in toluene. Then the thiol **3** was reacted with bromide **5** in the presence of Et₃N and afforded compound **1**, and **6–19**. Other bases were tested and some byproducts were produced, which gave rise to low yields.

The amide derivatives **20–27** were prepared in one step from INZ (**1**) in the presence of organic bases as depicted in Figure 4.

The amine derivative **28** was synthesized from INZ (**1**) and ethyl bromoacetate in the presence of K₂CO₃, which was depicted in Figure 7. Other organic bases, such as Et₃N or DIPEA, were tested and the reaction proceeded very slowly with low yields. Compound **28** was hydrolyzed by 1 M NaOH and afforded the acid **29**. The alcohol **30** was obtained through reduction of **28** by NaBH₄. LiBH₄ was tested and several byproducts were produced as revealed by TLC analysis. Figure 8 shows the “click chemistry” for the synthesis of triazol derivatives. Triazols **34–36** were obtained in good yields through the reaction of azide derivative and the propargyl **31** and **32** under the standard conditions [13].

Biological assessments of INZ analogs

The synthetic analogs were then assayed for their potential to induce p53 level and activity in H460 cells and HCT116^{+/+} cells by IB. Compounds were added into cultured H460 and HCT116^{+/+} cells at 0.5, 2, 10 μM for 18 hrs and harvested for IB. The p53 activation was assessed by up-regulating the levels of MDM2, p53 and p53 acetylation. The induction level of p53 by each of the tested INZ analogs was normalized against the loading control of GAPDH and compared to the level of p53 in the cells treated with 2 μM INZ (Figure 9). Compounds showing good efficacy in p53 induction were further subjected to a 3-day WST assay to assess their ability to kill cancer cells. INZ was used along with the analogs as a positive control in each assay. The EC₅₀ values for their ability to inhibit cell growth were calculated through serial dilution of their concentrations with the highest concentration at 50 μM in H460 and HCT116^{+/+} cells or 100 μM in H1299 and HCT116^{-/-} cells. Four-parameter or two-parameter Hill equation was employed to calculate and plot the dose-response curves as shown with some representative compounds in Figure 10. EC₉₀ values were calculated from the EC₅₀ and Hill slope by a web-based calculator: <http://www.graphpad.com/quickcalcs/Ecanything1.cfm>.

Anti-proliferative Effect of Synthetic INZ analogs

In synthetic INZ analogs containing triazino[5,6-b]indole (G1), subtle and major modifications to phenothiazine ring (G2) generally led to less potent molecules. Though subtle changes on the branches of the phenothiazine ring were tolerated (for instance, compounds **6** and **7** with chlorine or methoxy remained active in p53 induction) (Figure 5 and Figure 9), they did not reach 50% p53 induction in H460 cells and HCT116^{+/+} cells at 2 μM. The removal of any ring of G2, as shown for compound **10–13** (Figure 5), caused loss of activity, and those compounds were essentially inactive (Figure 9). The exception to this trend

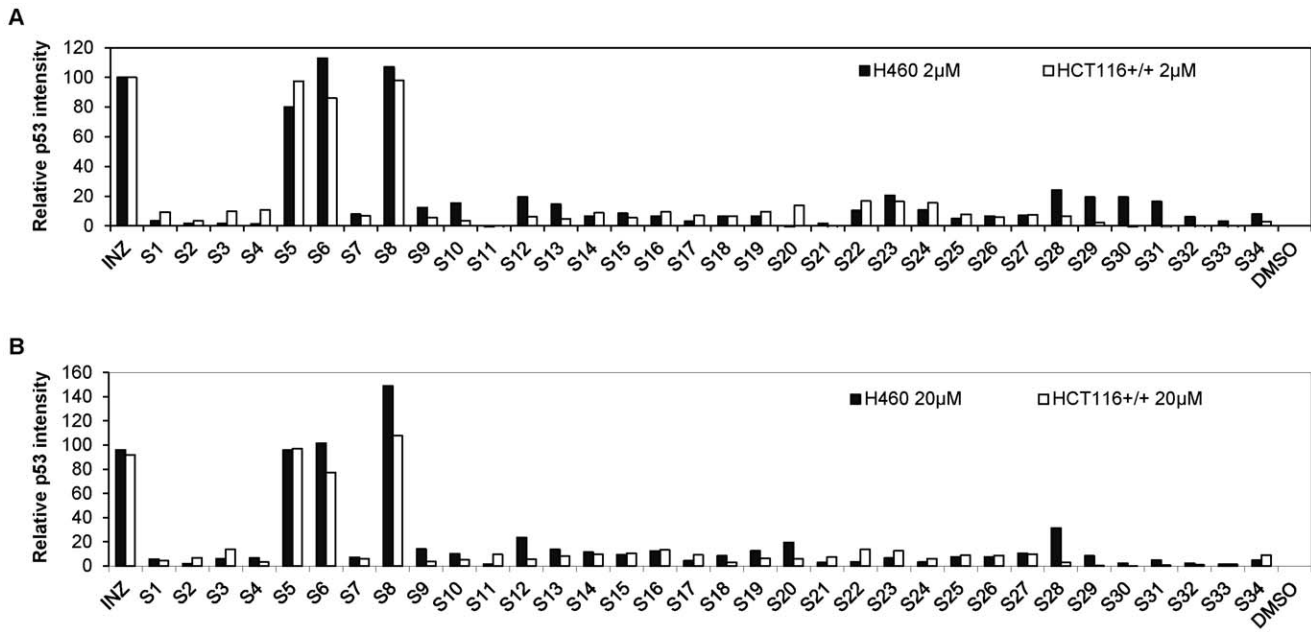


Figure 2. Cellular Activity of INZ Analogs S1–S34. (A–B) Initial Inauhizin analogs were purchased and tested the activity on H460 and HCT116^{+/+} by immunoblotting (IB). Cells were treated with the compounds at 2 μM or 20 μM for 18 hrs and harvested for IB and their p53 induction activity as quantified from IB data as shown in (A–B). doi:10.1371/journal.pone.0046294.g002

was substitution of the sulfur atom with methylene (**8**), 1-acridin-INZ derivative (**8**) drastically induced p53 at 0.5 μM, whereas compound **9**, whose sulfur was substituted with oxygen, was inactive (**Figure 9**). It should be noted that 1-acridin-INZ (**8**) also exhibited more than 2 fold higher potency than did INZ in its inhibitory effect on H460 ($EC_{50} = 2.7 \mu\text{M}$) (**Figure 10**) and HCT116^{+/+} cells ($EC_{50} = 1.3 \mu\text{M}$) (**Figure 10**). The EC_{90} values of this analog were in the range of 3.5–10 μM, which were 3–10 fold lower than those for INZ.

Compound **14** (**Figure 5**) with the longer chain containing butyl at R₁ position exhibited lower activity for p53 induction, which further indicated that the appropriate length of alkyl chain at R₁ position is crucial for the activity of INZ, as INZ activity in p53 activation was reduced or lost when the chain was either longer than 2 carbons (**14**, **Figure 5**) or removed (**S1–S3**, **Figure 3**). Compounds **15–19** (**Figure 5**) were synthesized to determine the effect of different substituents, such as electron-withdrawing group (halogen atoms) and electron donating group (methyl or methoxy), at R₃ position of indole ring (G1) on p53 induction. Compounds **16** and **17**, which have a chlorine and bromine atom, respectively, exhibited similar activity to that of INZ in HCT116^{+/+} cells with a dose-dependent induction of p53 acetylation at lysine 382, p53 protein level and the up-regulation of MDM2 level (**Figure 9**). Compound **18** with a methoxy group displayed a marked decrease in p53 activation. In contrast, the methyl derivative **19** exhibited a significant effect on p53 induction compared to INZ at 0.5 μM. It also inhibited the proliferation of H460 and HCT116^{+/+} with EC_{90} values of ~20–30 μM, which were 1.5 fold lower than that for INZ (**Figure 10C**). These results indicate that the order of influence of these substituents on the antiproliferative activity of INZ is as follows: $\text{CH}_3 > \text{Cl} > \text{Br} > \text{F} > \text{OCH}_3$.

The results from our preliminary biological screening of INZ analogs (**S5–S8**, **Figure 3**) suggested that R₂ position could be modified. We conjugated biotin directly to INZ through the formation of the amide bond at the active hydrogen of R₂ and

gained compound **20** (**Figure 5**). This biotin-conjugated INZ was initially designed for target identification studies. To our delight, the biotinylated INZ (**20**) was as effective as INZ in the induction of p53 acetylation and level in both H460 and HCT116^{+/+} cells [10] (**Figure 9B**). Another biotin-conjugated compound derived from the inactive compound **15** was used as a negative control in the target identification screening (data not shown). In addition to compound **20**, some other amide compounds (**21–27**) (**Figure 5**) were made through the same procedure. All these compounds with various ketone substitutions on R₂ exhibited good activities in p53 induction and cell growth inhibition in comparison with INZ (**Figure 9** and **10**). Derivatives **20**, **21** and **27** showed similar EC_{90} values of 7.5, 9.6 and 9.0 μM, respectively whereas INZ is about 39.9 μM. Removal (**25→32**, **Figure 5**) or separation (**21→33**, **Figure 5**) of the carbonyl group from the indol resulted in a significant decrease in activity (**Figure 9**). Replacing the ketone with an ester (**28**) or carboxylic acid (**29**) resulted in essentially inactive analogs, in striking contrast to its alcohol derivative **30**, which was comparable to compound **8** in p53 activation and cell growth inhibition (**Figure 5**, **9**, and **10**). The EC_{90} values of compound **30** as tested in H460 and HCT116^{+/+} cells, respectively, were ~7.7 μM and 4.6 μM, which was 5 fold lower than that of INZ (**Figure 10**). Since compounds **8** and **30** displayed more potent activity compared to INZ, we synthesized the analog **37** that contains both substitution of the sulfur atom with methylene on G2 and alcohol substitution on G1. We found that compound **37** was remarkably 10- and 5-fold more active than was INZ in growth inhibition of H460 and HCT116^{+/+} cells ($EC_{50} = 0.7 \mu\text{M}$ and 0.5 μM), respectively.

INZ displayed much higher toxicity to p53-containing human cancer cells than to p53-null cancer cells. This was evident in the EC_{50} and EC_{90} values, which were 1.5 and 5–7 fold greater in p53-null cells than in p53-containing cell lines, respectively (**Figure 10C**). We further examined the activity of INZ synthetic analogs by conducting in vitro cytotoxicity assays using p53 null lung cancer H1299 cells and colon cancer HCT116^{-/-} cells.

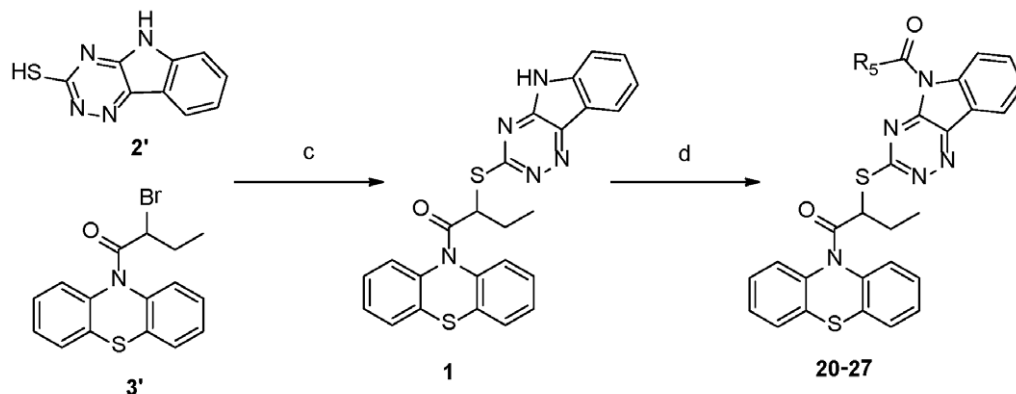
| ID | R ₁ | R ₂ | R ₃ | R ₄ | ID | R ₁ | G ₁ | ID | R ₁ | R ₂ | G ₂ | ID | R ₁ | G ₁ | G ₂ |
|-----|---------------------------------|---|----------------|----------------|-----|---------------------------------|----------------|-----|---------------------------------|---------------------------------|----------------|-----|-----------------------------------|----------------|----------------|
| INZ | CH ₂ CH ₃ | H | H | H | S9 | CH ₂ CH ₃ | | S19 | CH ₂ CH ₃ | H | | S29 | H | | |
| S1 | H | H | H | F | S10 | CH ₂ CH ₃ | | S20 | CH ₂ CH ₃ | H | | S30 | H | | |
| S2 | H | H | H | H | S11 | H | | S21 | CH ₂ CH ₃ | H | | S31 | CH(CH ₃) ₂ | | |
| S3 | H | CH ₃ | H | H | S12 | H | | S22 | CH ₂ CH ₃ | CH ₃ | | S32 | H | | |
| S4 | CH ₂ CH ₃ | CH ₃ | Br | H | S13 | H | | S23 | CH ₃ | H | | S33 | CH ₃ | | |
| S5 | CH ₂ CH ₃ | CH ₃ | H | H | S14 | H | | S24 | CH ₃ | H | | S34 | CH ₃ | | |
| S6 | CH ₂ CH ₃ | CH ₂ CH ₃ | H | H | S15 | H | | S25 | CH ₃ | H | | | | | |
| S7 | CH ₂ CH ₃ | CH ₂ CH ₂ CH ₃ | H | H | S16 | H | | S26 | CH ₃ | H | | | | | |
| S8 | CH ₂ CH ₃ | CH ₂ CH=CH ₂ | H | H | S17 | H | | S27 | H | CH ₂ CH ₃ | | | | | |
| | | | | | S18 | H | | S28 | H | H | | | | | |

Figure 3. Table of Chemical Structures of Representative Commercial Analogs S1–S34.

doi:10.1371/journal.pone.0046294.g003

Compounds **8**, **19**, **21**, **30** and **37** were demonstrated much less effective in H1299 cells and HCT116^{-/-} cells, in contrast to their inhibitory activity on p53-containing cells (**Figure 10C**), as the

EC₅₀ values of compounds **8**, **30** and **37** on H1299 were 10.4, 16.6 and 11.2 μM, respectively, which were 3–15 fold higher than those on H460 cells. The EC₉₀ values of compound **8**, **30** and **37**



(c) **5**, Et₃N, DMF, rt (d) acid chloride, Et₃N or DIPEA, THF, rt

Figure 4. Synthesis of INZ Analogs 20–27.

doi:10.1371/journal.pone.0046294.g004

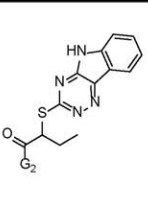
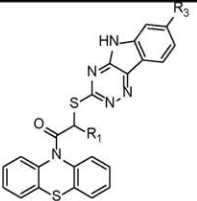
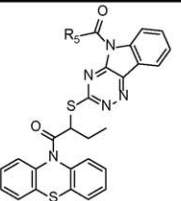
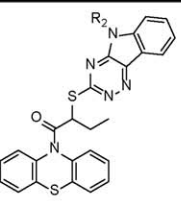
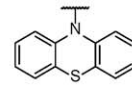
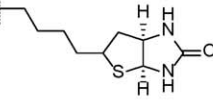
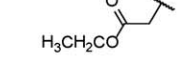
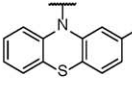
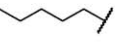
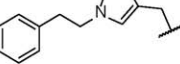
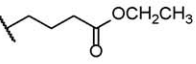
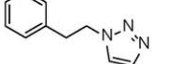
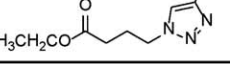
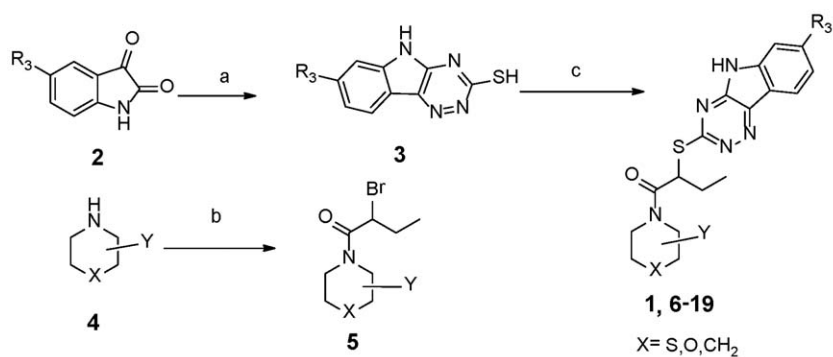
|  | |  | |  | |  | | |
|---|---|---|---|--|------|--|------|---|
| Cmpd | G2 | Cmpd | R ₁ | R ₃ | Cmpd | R ₅ | Cmpd | R ₂ |
| 6 |  | 14 | CH ₂ CH ₂ CH ₂ CH ₃ | H | 20 |  | 28 |  |
| 7 |  | 15 | CH ₂ CH ₃ | F | 21 |  | 29 |  |
| 8 |  | 16 | CH ₂ CH ₃ | Cl | 22 |  | 30 |  |
| 9 |  | 17 | CH ₂ CH ₃ | Br | 23 |  | 31 |  |
| 10 |  | 18 | CH ₂ CH ₃ | OCH ₃ | 24 |  | 32 |  |
| 11 |  | 19 | CH ₂ CH ₃ | CH ₃ | 25 |  | 33 |  |
| 12 |  | | | | 26 |  | 34 |  |
| 13 |  | | | | 27 |  | 35 |  |
| | | | | | | | 36 |  |

Figure 5. Table of Chemical Structures of INZ Synthetic Analogs 6–36.

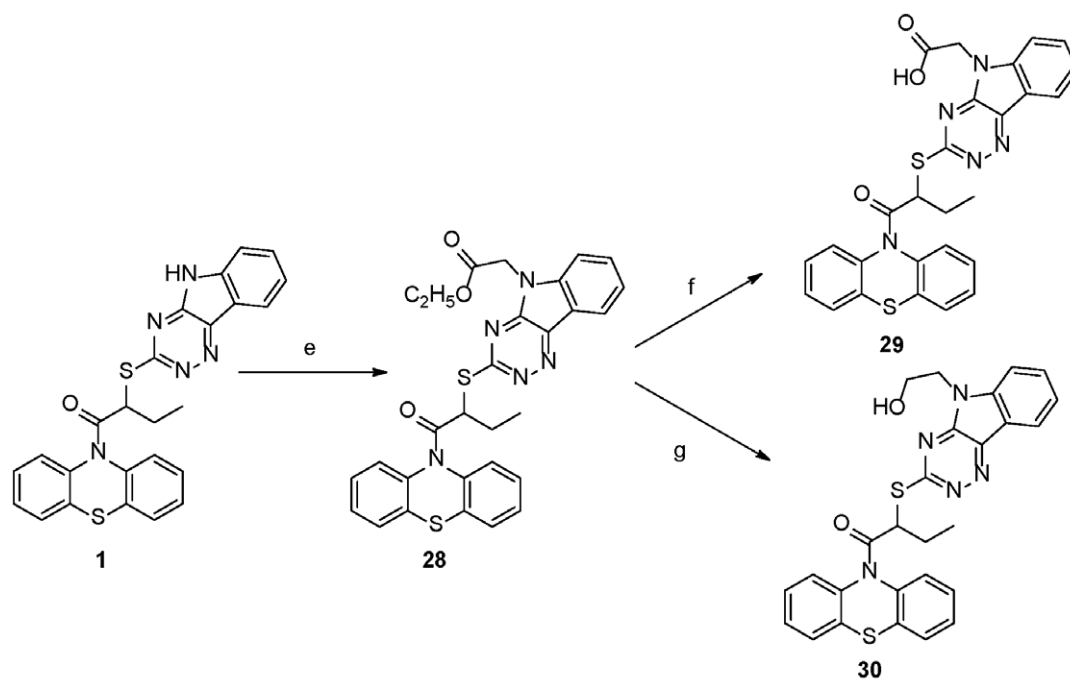
doi:10.1371/journal.pone.0046294.g005



(a) Thiosemicarbazide, H₂O, 100 °C; (b) 2-Bromobutyl bromide, toluene, reflux; (c) 5, Et₃N, DMF, rt

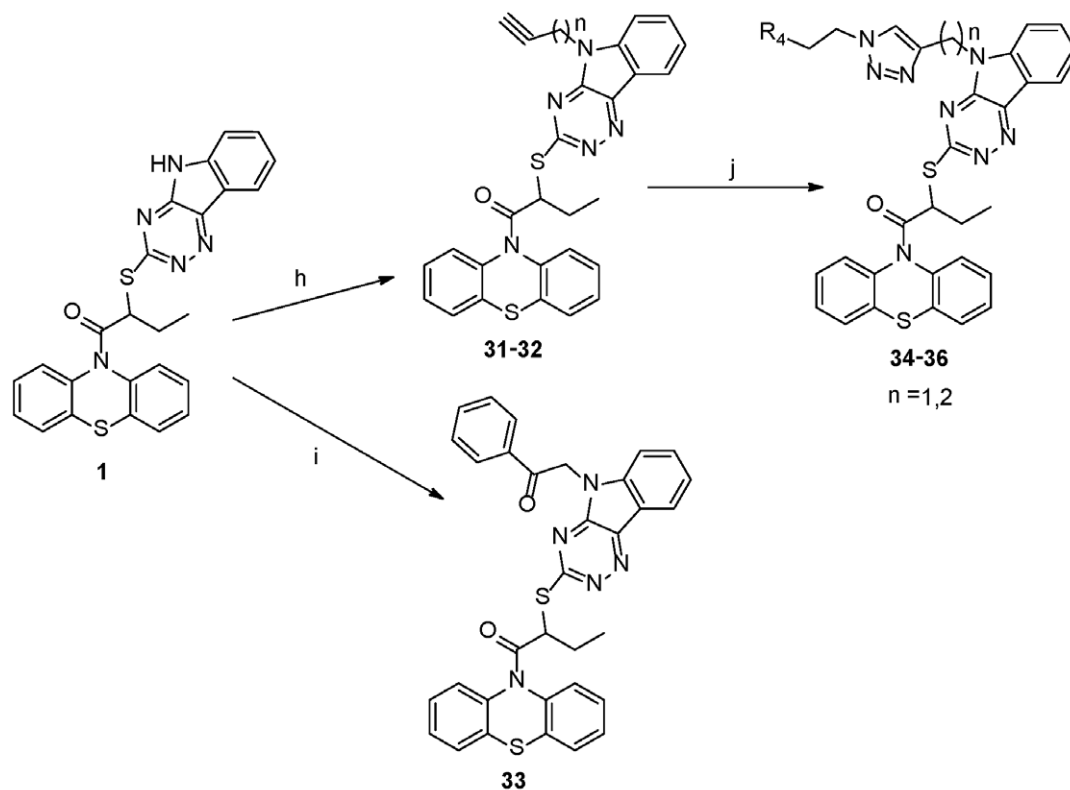
Figure 6. Synthesis of INZ Analogs 6–19.

doi:10.1371/journal.pone.0046294.g006



(e) Ethyl bromoacetate, K₂CO₃, DMF, rt; (f) 1 M NaOH, 1,4-dioxane, rt; (g) NaBH₄, THF, rt

Figure 7. Synthesis of INZ Analogs 28–30.
doi:10.1371/journal.pone.0046294.g007



(h) Propargyl bromide or 4-bromo-1-butyne, K₂CO₃ or Cs₂CO₃, DMF, rt; (i) 2-bromoacetophenone, K₂CO₃, DMF, rt; (j) azide derivative, sodium ascorbate, CuSO₄, *t*-BuOH/H₂O, 55°C

Figure 8. Synthesis of INZ Analogs 31–36.
doi:10.1371/journal.pone.0046294.g008

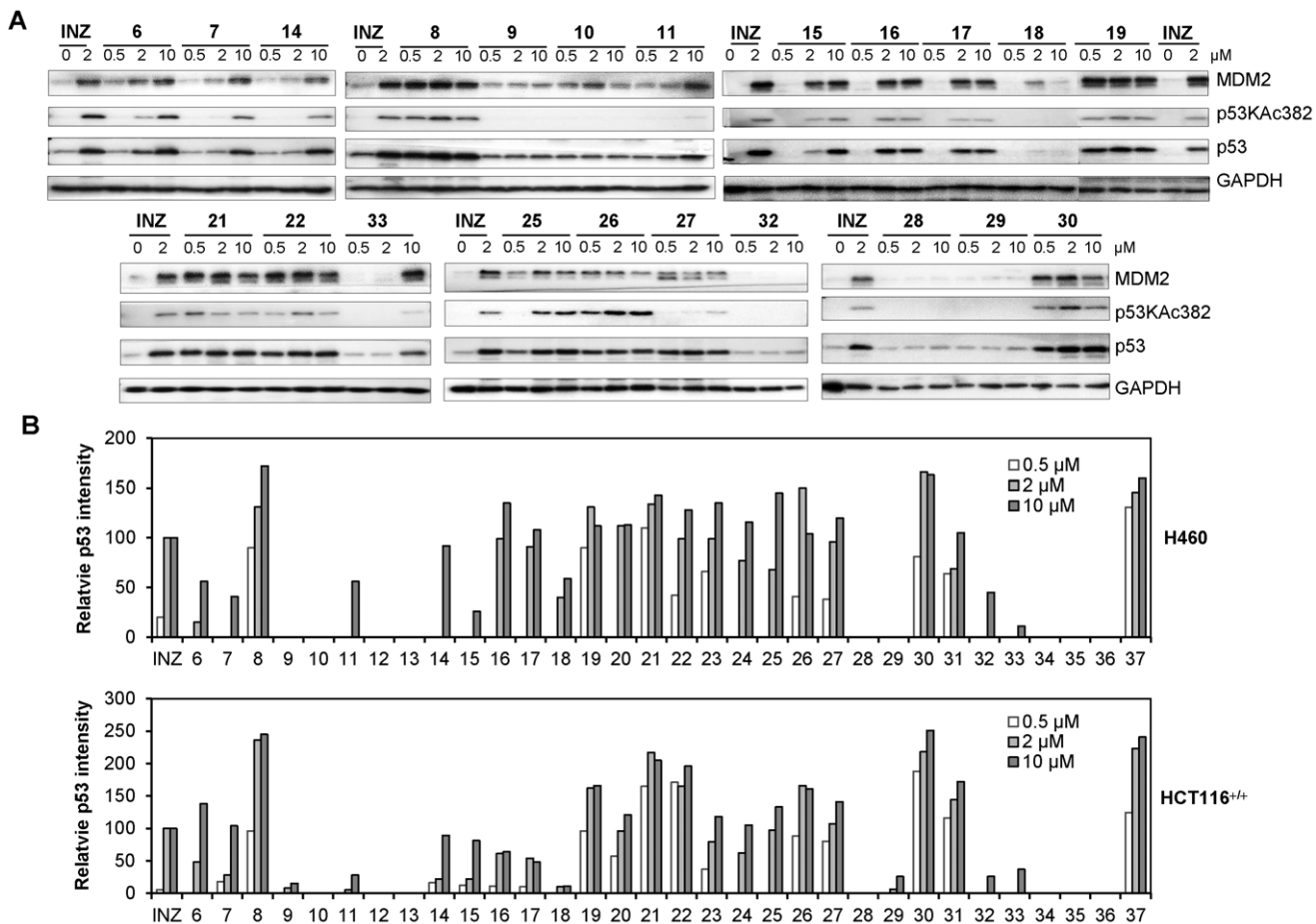


Figure 9. Cellular Activities of INZ Synthetic Analogs 6–37. (A–B) Cellular activity of INZ synthetic analogs 6–37 measured using IB that detects p53 levels and activity in H460 and HCT116^{+/+} cells. Cells were harvested for IB with antibodies as indicated after being treated with each compound for 18 hrs as shown in representative blots from HCT116^{+/+} cells (A) (number denotes each compound; Inauhizin, INZ), and their p53 induction activity as quantified from IB data as shown in (B). doi:10.1371/journal.pone.0046294.g009

on H1299 cells and HCT116^{-/-} cells were greater than 50 μM whereas those on H460 and HCT116^{+/+} cells were 3.5 and 10, 7.7 and 4.6, and 3.6 and 5.0 μM, respectively. More remarkably, these synthetic analogs were much less toxic to normal human fibroblast cell WI-38 (Figure 10C), while they were much more potent than was INZ in killing p53-containing cancer cells. For example, the EC₅₀ value of compound 37 for WI-38 was unable to be determined at the highest concentration tested (50 μM) in comparison of its EC₅₀ values of 0.7 and 0.5 μM to p53-containing H460 and HCT116^{+/+} cells, respectively. Together, these results indicate that these more potent INZ analogs, such as compounds 8, 30 and 37, possess strong p53-dependent cytotoxicity. Among them, compound 37 stands out as the most effective INZ analog from this study.

Conclusion

Our initial studies on the 46 commercial analogs of INZ yielded information on the important functional groups at each of its two scaffolds identified as triazino[5,6-b]indol ring (G1) and phenothiazine ring (G2). The functional analyses of the commercial and synthetic analogs of INZ for their ability to activate p53 and to inhibit cell growth further as described above validate that each of the functional groups of INZs is critical for p53 activation and

inhibition of cancer cell growth (Figure 11). Most modifications to phenothiazine ring G2, such as the branch substitutions (6–7), or replacement with other rings (9–13, S19–S22), led to the decreased activity in p53 induction, with the exception of that the substitution of sulfur in the G2 region by methylene (1→8) showed greater potency than compound 1 in both p53 induction and cancer cell inhibition. Analyses of analogs S1–S3, and 14 demonstrate that the ethyl group at R₁ is required for the activity of these compounds. The butyl group was tolerated. Modification of R₃ position at the region G1 with methyl, but not halide or methoxy substitutions, increased activity in both of the assays (15–19). Most modifications on R₂ at the G1 region resulted in the impressive improvement in terms of p53 activation compared to compound 1 (20–27, 30–31). Overall, the best compound from this study was 1-acridin-INZ alcohol (37). The potency of this analog, compared to INZ, was improved nearly 5- to 10-fold in cancer growth inhibition. Interestingly and importantly, compounds 8, 30 and 37 were more potent in p53 activation than their parental compound INZ especially with the selective toxicity to p53-containing tumor cells, but not to normal cells.

Based on these SAR and cell-based analyses as described here, 1-acridin-INZ alcohol (37) represented the most promising candidate for further development and will be selected for further

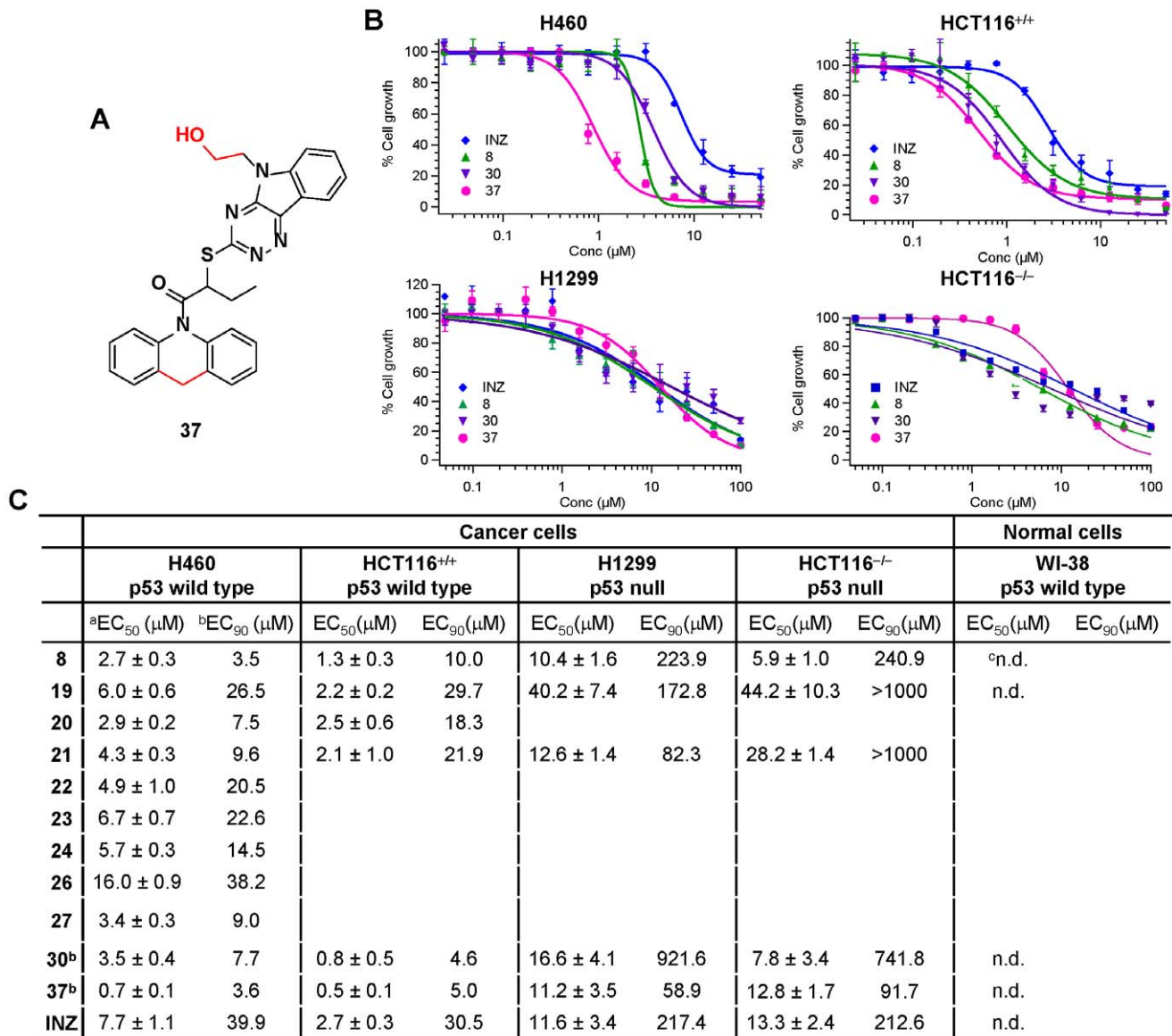


Figure 10. Cell Growth Inhibition by INZ Synthetic Analogs. (A) Structure of INZ synthetic analog **37**. (B) Representative cell growth inhibition curves of INZ synthetic analogs **8**, **30** and **37** in H460, H1299, HCT116^{+/+} and HCT116^{-/-} cell lines. (C) ^aEC₅₀ of the selected INZ analogs represent the average of triplicates. The EC₅₀ values were determined by the two-parameter Hill equation where EC₅₀ and the Hill coefficient were allowed to refine while the maximal and minimal values remain fixed. ^bEC₉₀ values were calculated from the EC₅₀ and Hill slope by a web-based calculator: <http://www.graphpad.com/quickcalcs/Ecanything1.cfm>. ^c Not be able to be determined. doi:10.1371/journal.pone.0046294.g010

characterization of its biological activity against cancer by using orthotopic lung tumors derived from H460 cells in the near future.

Materials and Methods

Compounds S1–S34

INZ analogs **S1–S34** were purchased from Asinex, ChemDiv and ChemBridge. Compounds **S1–S5** were described in a preceding paper, re-validated by LC/MS on an Agilent 1200 LC/MS system (Agilent Technology) at the Chemical Genomics Core Facility of Indiana University School of Medicine. The minimum purity of all compounds is higher than 90%.

Cell Culture and Immunoblotting Analysis

Human lung carcinoma H460, non-small-cell lung cancer H1299, human colon cancer HCT116 (HCT116^{+/+}), and human embryonic fibroblast WI-38 were bought from the American Type Culture Collection (ATCC). Human colon cancer HCT116 p53 null cell lines (HCT116^{-/-}) were generously offered by Dr. Bert Vogelstein (Johns Hopkins University) [14]. Those cell lines were cultured in Dulbecco's modified Eagle's medium supplemented with 10% fetal bovine serum, 100 U per mL penicillin, and 100 U per mL streptomycin. Compounds were dissolved in DMSO and diluted directly into the medium to the indicated concentrations; 0.1% DMSO was used as a control. After incubation with the compounds for 18 h, cells were harvested and lysed in 50 mM Tris-HCl pH 8.0, 150 mM NaCl, 5 mM EDTA, 0.5% NP-40 supplemented with 1 mM DTT and 0.2 mM PMSF. An equal

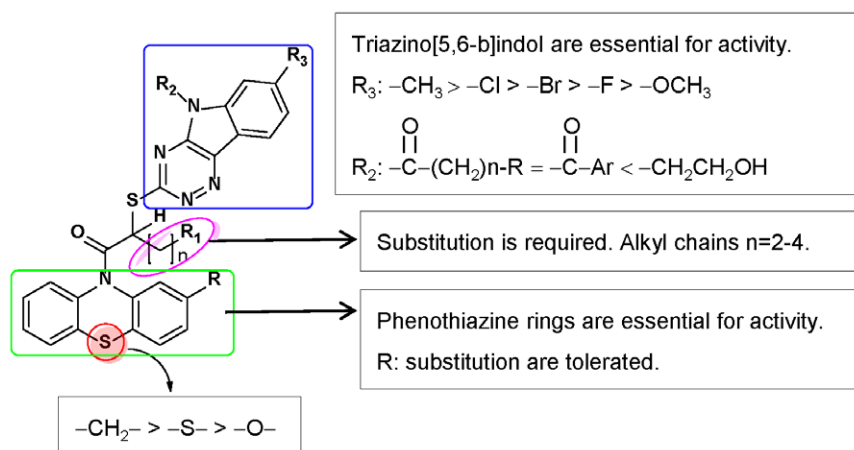


Figure 11. Structure-Activity Relationships of INZ.

doi:10.1371/journal.pone.0046294.g011

amount of protein samples (50 μ g) was subjected to SDS-PAGE and transferred to a PVDF membrane (PALL Life Science). The membranes with transferred proteins were blocked with 1 \times TBST containing 5% non-fat, dried milk for 1 h at room temperature, and then incubated with anti-p53-acetylated (lys382, Cell Signaling), anti-p53 (mouse monoclonal, DO-1, Santa Cruz), anti-MDM2 (4B11) [15], or anti-GAPDH antibodies (Sigma) followed by a secondary antibody labeled with horseradish peroxidase (Pierce). The blots were developed by an enhanced chemiluminescence detection kit (Thermo Scientific), and signals were visualized by Omega 12iC Molecular Image System (UltraLUM).

Cell Viability Assay

To assess cell growth, the cell counting kit (Dojindo Molecular Technologies Inc., Gaithersburg, Maryland) was used according to manufacturer's instructions. Cell suspensions were seeded at 3,000 cells per well in 96-well culture plates and incubated overnight at 37°C. Compounds were added into the plates and incubated at 37°C for 72 hrs. Cell growth inhibition was determined by adding WST-8 at a final concentration of 10% to each well, and the absorbance of the samples was measured at 450 nm using a Microplate Reader (Molecular Device, SpectraMax M5⁵). EC₅₀ values were determined by the Hill equation using Igor 4.01 (Lake Oswego, Oregon, USA). EC₉₀ values were calculated from the EC₅₀ and Hill slope by a web-based calculator: <http://www.graphpad.com/quickcalcs/Ecanything1.cfm>.

General Chemistry

All purchased chemicals were reagent-grade or better. Proton and carbon NMR spectra were recorded on a 500 MHz Bruker Avance II spectrometer. Chemical shifts are reported in δ (parts per million, ppm) with the δ 7.26 signal of CDCl₃ (¹H NMR), δ 2.50 signal of DMSO-*d*₆ (¹H NMR), or δ 77.2 signal of CDCl₃ (¹³C NMR) as internal standards. All column chromatography was performed using Dynamic Adsorbents 230–400 mesh silica gel (SiO₂) with the indicated solvent system unless otherwise noted. TLC analysis was performed using 254 nm glass-backed plates and visualized using UV light (254 nm). HRMS data were obtained at the Mass Spectrometry Facility at IUPUI Chemistry Department on a Waters/Macromass LCT. All the synthetic compounds were analyzed by LC/MS on an Agilent 1200 LC/MS system (Agilent Technology) at the Chemical Genomics Core

Facility of Indiana University School of Medicine and the purity was over 95%.

General procedure for synthesis of compounds 1, 6–19

2-((5H-[1,2,4]triazino[5,6-b]indole-3-yl)thio)-1-(10H-phenothiazin-10-yl)butan-1-one (1, INZ). 2-bromo-1-(10H-phenothiazin-10-yl)butan-1-one (3.675 g, 25 mmol) and 5H-[1,2,4]triazino[5,6-b]indole-3-thiol (2.125 g, 25 mmol) were dissolved in 50 ml anhydrous DMF and cooled to 0°C. 11.1 ml Et₃N (250 mmol) was dropped to the above mixture. After stirring for 1.5 h, TLC indicated that the reaction was completed and stopped. 300 ml ethyl acetate was added to the reaction mixture. The organic phase was washed by saturated NH₄Cl for five times and separated. It was dried by anhydrous Na₂SO₄ and filtered. The organic phase was concentrated to about 15 ml and the pale solid was formed. The amorphous solid was collected and washed by a few ethyl acetate. ¹H NMR (500 MHz, DMSO-*d*₆) δ : 12.63 (br, 1H), 8.34 (d, $J=7.5$, 1H), 7.89–7.96 (m, 1H), 7.56–7.73 (m, 4H), 7.37–7.47 (m, 5H), 7.29–7.22 (m, 1H), 5.27 (t, $J=7.0$, 1H), 1.86 (br, 1H), 1.74 (br, 1H), 0.85 (br, 3H). ¹³C NMR (125 MHz, DMSO-*d*₆) δ : 170.0, 146.8, 141.7, 140.9, 138.5, 138.3, 131.4, 128.6, 128.2, 128.0, 127.7, 127.4, 123.0, 122.0, 118.0, 113.2, 31.1, 25.9, 11.8. HRMS was calculated for C₂₅H₁₉N₅O₂ 469.1031 and found 469.1047.

2-((5H-[1,2,4]triazino[5,6-b]indol-3-yl)thio)-1-(2-chloro-10H-phenothiazin-10-yl)butan-1-one (6). Compound **6** was synthesized similarly to **1**. ¹H NMR (500 MHz, DMSO-*d*₆) δ : 12.64 (d, $J=17.5$, 1H), 8.33–8.35 (m, 1H), 7.84–7.91 (m, 1H), 7.60–7.34 (m, 4H), 7.39–7.48 (m, 5H), 5.15–5.26 (m, 1H), 1.82 (br, 1H), 1.73 (br, 1H), 0.85 (br, 3H). HRMS calcd for C₂₅H₁₈ClN₅O₂ 503.0641; found 503.0643.

2-((5H-[1,2,4]triazino[5,6-b]indol-3-yl)thio)-1-(2-methoxy-10H-phenothiazin-10-yl)butan-1-one (7). Compound **7** was synthesized similarly to **1**. ¹H NMR (500 MHz, DMSO-*d*₆) δ : 12.65 (d, $J=22.5$, 1H), 8.32–8.35 (m, 1H), 7.59–7.73 (m, 1H), 7.36–7.53 (m, 7H), 7.21 (br, 1H), 6.96–7.21 (m, 1H), 5.29 (t, $J=7.0$, 1H), 3.51–3.71 (m, 3H), 1.95 (br, 1H), 1.77 (br, 1H), 0.86 (br, 3H). HRMS calcd for C₂₆H₂₁N₅O₂S₂ 499.1137; found 499.1144.

2-((5H-[1,2,4]triazino[5,6-b]indol-3-yl)thio)-1-(acridin-10(9H)-yl)butan-1-one (8). Compound **8** was synthesized similarly to **1**. ¹H NMR (500 MHz, DMSO-*d*₆) δ : 12.60 (br, 1H), 8.32 (d, $J=7.5$, 1H), 7.68–7.73 (m, 3H), 7.59 (d, $J=8.0$, 1H), 7.44–7.47 (m, 1H), 7.17–7.34 (m, 6H), 5.41 (s, 1H), 3.86 (s, 2H), 2.10 (br, 1H), 1.86 (br, 1H), 0.95 (br, 3H). ¹³C NMR (125 MHz,

DMSO- d_6) δ 169.9, 166.1, 146.7, 141.8, 140.9, 139.2, 135.2, 131.4, 127.8, 126.7, 126.6, 125.5, 122.9, 122.0, 117.9, 113.2, 47.3, 33.4, 26.2, 11.9. HRMS calcd for $C_{26}H_{21}N_5OS$ 451.1467; found 451.1474.

2-((5*H*-[1,2,4]triazino[5,6-*b*]indol-3-yl)thio)-1-(10*H*-phenothiazin-10-yl)butan-1-one (9). Compound **9** was synthesized similarly to **1**. 1H NMR (500 MHz, DMSO- d_6) δ 12.63 (br, 1H), 8.33 (d, $J=8.0$, 1H), 7.70–7.34 (m, 3H), 7.60 (d, $J=8.0$, 1H), 7.46 (d, $J=7.5$, 1H), 7.19–7.25 (m, 6H), 5.47 (t, $J=7.0$, 1H), 1.99–2.03 (m, 1H), 1.81–1.86 (m, 1H), 0.89 (t, $J=7.5$, 3H). HRMS calcd for $C_{27}H_{19}N_5O_2S$ 453.1259; found 453.1270.

2-((5*H*-[1,2,4]triazino[5,6-*b*]indol-3-yl)thio)-1-(2*H*-benzo[*b*] [1,4]thiazin-4(3*H*)-yl)butan-1-one (10). Compound **10** was synthesized similarly to **1**. 1H NMR (500 MHz, $CDCl_3$) δ 10.15 (s, 1H), 8.38 (d, $J=7.5$, 1H), 7.60–7.66 (m, 3H), 7.43 (t, $J=7.5$, 1H), 7.23 (br, 1H), 7.12–7.14 (m, 2H), 5.30 (br, 1H), 3.30 (br, 3H), 2.14 (d, $J=7.0$, 1H), 2.00 (br, 2H), 1.08 (br, 3H). HRMS calcd for $C_{21}H_{19}N_5OS_2$ 421.1031; found 421.1038.

2-((5*H*-[1,2,4]triazino[5,6-*b*]indol-3-yl)thio)-1-(3,4-dihydroquinolin-1(2*H*)-yl)butan-1-one (11). Compound **11** was synthesized similarly to **1**. 1H NMR (500 MHz, DMSO- d_6) δ 12.60 (br, 1H), 7.69–7.72 (m, 1H), 7.58 (d, $J=8.0$, 1H), 7.45 (t, $J=7.0$, 1H), 7.35 (br, 1H), 7.12–7.16 (m, 2H), 7.06 (t, $J=7.5$, 1H), 5.28 (t, $J=6.5$, 1H), 3.97 (br, 1H), 3.55 (br, 1H), 2.64–2.76 (m, 2H), 2.04 (br, 2H), 1.86 (br, 2H), 0.89 (br, 3H). HRMS calcd for $C_{22}H_{21}N_5OS$ 403.1467; found 403.1479.

2-((5*H*-[1,2,4]triazino[5,6-*b*]indol-3-yl)thio)-1-thiomorpholinobutan-1-one (12). Compound **12** was synthesized similarly to **1**. 1H NMR (500 MHz, $CDCl_3$) δ 10.88 (br, 1H), 8.37 (d, $J=8.0$, 1H), 7.63–7.64 (m, 2H), 7.40–7.43 (m, 1H), 5.35 (t, $J=7.0$, 1H), 4.12–4.19 (m, 2H), 4.03–4.05 (m, 1H), 3.86–3.89 (m, 1H), 2.92–2.95 (m, 1H), 2.72–2.77 (m, 1H), 2.60–2.64 (m, 2H), 2.19–2.26 (m, 1H), 2.04–2.10 (m, 1H), 1.13 (t, $J=7.0$, 3H). HRMS calcd for $C_{17}H_{19}N_5OS_2$ 373.1031; found 373.1033.

2-((5*H*-[1,2,4]triazino[5,6-*b*]indol-3-yl)thio)-1-(2,3-dihydro-1*H*-pyrrolo[3,2-*b*]pyridine-1-yl)butan-1-one (13). Compound **13** was synthesized similarly to **1**. 1H NMR (500 MHz, DMSO- d_6) δ 12.56 (s, 1H), 8.28 (d, $J=8.0$, 1H), 8.08 (d, $J=4.5$, 1H), 7.67–7.71 (m, 2H), 7.56 (d, $J=8.5$, 1H), 7.42 (t, $J=7.5$, 1H), 7.00–7.03 (m, 1H), 6.59 (br, 1H), 4.05 (t, $J=8.5$, 2H), 3.12 (q, $J=7.5$, 2H), 2.10–2.15 (m, 1H), 1.98–2.04 (m, 1H), 1.07 (t, $J=7.5$, 3H). HRMS calcd for $C_{20}H_{18}N_6OS$ 390.1263; found 390.1274.

2-((5*H*-[1,2,4]triazino[5,6-*b*]indol-3-yl)thio)-1-(10*H*-phenothiazin-10-yl)hexan-1-one (14). Compound **14** was synthesized similarly to **1**. 1H NMR (500 MHz, DMSO- d_6) δ 12.62 (br, 1H), 8.35 (d, $J=7.5$, 1H), 7.96 (br, 1H), 7.58–7.74 (m, 4H), 7.37–7.48 (m, 5H), 7.26 (br, 1H), 5.32 (t, $J=7.0$, 1H), 1.86 (br, 1H), 1.83 (br, 1H), 1.09–1.24 (m, 4H), 0.73 (br, 3H). HRMS calcd for $C_{27}H_{23}N_5OS_2$ 497.1344; found 497.1348.

2-((7-fluoro-5*H*-[1,2,4]triazino[5,6-*b*]indol-3-yl)thio)-1-(10*H*-phenothiazin-10-yl)butan-1-one (15). Compound **15** was synthesized similarly to compound **1**. 1H NMR (500 MHz, DMSO- d_6) δ 12.70 (br, 1H), 8.17 (d, $J=7.0$, 1H), 7.89 (br, 1H), 7.56–7.64 (m, 4H), 7.37–7.43 (m, 4H), 7.22–7.25 (m, 1H), 5.26 (t, $J=7.0$, 1H), 1.95 (br, 1H), 1.74 (br, 1H), 0.85 (d, $J=7.0$, 3H). HRMS calcd for $C_{25}H_{18}FN_5OS_2$ 487.0937; found 487.0962.

2-((7-chloro-5*H*-[1,2,4]triazino[5,6-*b*]indol-3-yl)thio)-1-(10*H*-phenothiazin-10-yl)butan-1-one (16). Compound **16** was synthesized similarly to **1**. 1H NMR (500 MHz, DMSO- d_6) δ 12.79 (br, 1H), 8.38 (s, 1H), 7.88 (br, 1H), 7.73–7.79 (m, 1H), 7.49–7.63 (m, 3H), 7.37–7.43 (m, 4H), 7.23 (br, 1H), 5.26 (t, $J=7.0$, 1H), 1.86 (br, 1H), 1.74 (br, 1H), 0.86 (br, 3H). HRMS calcd for $C_{25}H_{18}ClN_5OS_2$ 503.0641; found 503.0641.

2-((7-bromo-5*H*-[1,2,4]triazino[5,6-*b*]indol-3-yl)thio)-1-(10*H*-phenothiazin-10-yl)butan-1-one (17). Compound **17** was synthesized similarly to **1**. 1H NMR (500 MHz, DMSO- d_6) δ 12.84 (br, 1H), 8.50 (s, 1H), 7.85 (d, $J=8.0$, 2H), 7.58 (d, $J=8.5$, 3H), 7.38–7.41 (m, 4H), 7.23 (br, 1H), 5.26 (s, 1H), 1.86 (br, 1H), 1.73 (br, 1H), 0.85 (br, 3H). HRMS calcd for $C_{25}H_{18}BrN_5OS_2$ 547.0136; found 547.0136.

2-((7-methoxy-5*H*-[1,2,4]triazino[5,6-*b*]indol-3-yl)thio)-1-(10*H*-phenothiazin-10-yl)butan-1-one (18). Compound **18** was synthesized similarly to **1**. 1H NMR (500 MHz, DMSO- d_6) δ : 12.47 (br, 1H), 7.89 (br, 1H), 7.85 (br, 1H), 7.52–7.64 (m, 4H), 7.37–7.43 (m, 3H), 7.32–7.34 (m, 1H), 7.22 (br, 1H), 5.25 (t, $J=7.0$, 1H), 1.86 (br, 1H), 1.74 (br, 1H), 0.85 (br, 3H). HRMS calcd for $C_{26}H_{21}N_5O_2S_2$ 499.1137; found 499.1136.

2-((7-methyl-5*H*-[1,2,4]triazino[5,6-*b*]indol-3-yl)thio)-1-(10*H*-phenothiazin-10-yl)butan-1-one (19). Compound **19** was synthesized similarly to **1**. 1H NMR (500 MHz, DMSO- d_6) δ 12.50 (br, 1H); 8.13 (s, 1H), 7.87 (br, 1H), 7.49–7.61 (m, 5H), 7.37–7.42 (m, 3H), 7.22 (br, 1H), 5.25 (d, $J=6.5$, 1H), 2.52 (s, 3H), 1.90 (br, 1H), 1.74 (br, 1H), 0.86 (br, 3H). HRMS calcd for $C_{26}H_{21}N_5OS_2$ 483.1188; found 483.1196.

General procedure for synthesis of compounds 20–27

5-(5-oxo-5-(3-((1-oxo-1-(10*H*-phenothiazin-10-yl)butan-2-yl)thio)-5*H*-[1,2,4]triazino[5,6-*b*]indol-5-yl)pentyl)tetrahydro-1*H*-thieno[2,3-*d*]imidazole-2(5*H*)-one (20). Biotin (100 mg, 0.410 mmol) was placed in 10 ml reaction flask and cooled to 0°C. 2.7 ml $SOCl_2$ was added to the flask and allowed to room temperature. The mixture was stirred for 1 h and excess $SOCl_2$ was evaporated. The residue was co-evaporated with 5 ml anhydrous toluene for three times to give the biotin acid chloride. The crude acid chloride was dissolved in 5 ml anhydrous THF. INZ (65 mg, 0.138 mmol) was dissolved in 3 ml anhydrous THF and injected to the above solution through syringe. The mixture was cooled to 0°C and 100 μ l Et_3N (0.717 mmol) was dropped to the mixture. The solution was then allowed to room temperature. TLC was used to monitor the reaction. After 11 h, TLC indicated that the reaction was completed. The reaction mixture was diluted with 30 ml ethyl acetate and washed by saturated NaCl for two times. The organic phase was separated and dried by anhydrous Na_2SO_4 . The organic phase was filtered, concentrated in vacuum and was purified by column (DCM/ CH_3OH , 55:1). The product was obtained as viscous oil. 1HNMR (500 MHz, $CDCl_3$) δ 8.69 (d, $J=8.5$, 1H), 8.40 (d, $J=7.5$, 1H), 7.92 (br, 1H), 7.75–7.72 (m, 1H), 7.67 (d, $J=7.0$, 1H), 7.59–7.56 (m, 1H), 7.53 (d, $J=3.0$, 1H), 7.40 (br, 1H), 7.35–7.29 (m, 3H), 7.18 (br, 1H), 5.60 (d, $J=39.5$, 1H), 5.42–5.38 (m, 1H), 5.14 (s, 1H), 4.56–4.53 (m, 1H), 4.41–4.37 (m, 1H), 3.48–3.41 (m, 1H), 3.35–3.26 (m, 1H), 3.25–3.23 (m, 1H), 2.98–2.95 (m, 1H), 2.76 (d, $J=12.5$, 1H), 1.90–1.83 (m, 4H), 1.79–1.75 (m, 1H), 1.70 (br, 1H), 1.61–1.58 (m, 2H), 0.98–0.90 (m, 3H). ^{13}C NMR (125 MHz, $CDCl_3$) δ 173.1, 170.0, 167.7, 163.7, 146.7, 142.4, 139.5, 138.5, 138.3, 132.2, 127.7, 127.5, 127.3, 127.0, 126.8, 125.9, 121.4, 119.6, 117.8, 62.0, 60.4, 55.4, 55.3, 40.6, 39.1, 28.5, 28.4, 26.0, 24.2, 11.7. HRMS calcd for $C_{35}H_{33}N_7O_3S_3$ 695.1807; found 695.1817.

2-((5-benzoyl-5*H*-[1,2,4]triazino[5,6-*b*]indol-3-yl)thio)-1-(10*H*-phenothiazin-10-yl)butan-1-one (21). Compound **21** was synthesized similarly to **20**. 1H NMR (500 MHz, DMSO- d_6) δ 8.49 (d, $J=7.5$, 1H), 8.23 (d, $J=8.5$, 1H), 7.60–7.78 (m, 6H), 7.40–7.55 (m, 4H), 7.17–7.28 (m, 4H), 7.06 (br, 1H), 4.89 (t, $J=6.5$, 1H), 1.93 (t, $J=6.5$, 1H), 1.57–1.62 (m, 1H), 0.75 (t, $J=7.0$, 3H). HRMS calcd for $C_{32}H_{23}N_5O_2S_2$ 573.1293; found 573.1298.

2-((5-nicotinoyl-5H-[1,2,4]triazino[5,6-b]indol-3-yl)thio)-1-(10H-phenothiazin-10-yl)butan-1-one (22). Compound **22** was synthesized similarly to **20**. ¹H NMR (500 MHz, CDCl₃) δ 8.97 (s, 1H), 8.91 (d, *J* = 4.0, 1H), 8.49 (d, *J* = 8.0, 1H), 8.41 (d, *J* = 8.5, 1H), 8.03–8.05 (m, 1H), 7.78–7.84 (m, 2H), 7.66 (t, *J* = 7.5, 1H), 7.58 (d, *J* = 7.0, 1H), 7.48–7.51 (m, 2H), 7.34 (br, 1H), 7.26–7.28 (m, 3H), 7.12 (br, 1H), 5.08 (t, *J* = 6.0, 1H), 1.94–1.96 (m, 1H), 1.67–1.70 (m, 1H), 0.83 (t, *J* = 6.5, 3H). ¹³C NMR (125 MHz, CDCl₃) δ 169.9, 167.7, 166.4, 153.8, 150.6, 146.7, 141.9, 139.3, 138.4, 138.2, 137.3, 132.0, 129.6, 128.2, 127.7, 127.3, 127.2, 127.1, 126.9, 126.7, 126.2, 123.1, 121.9, 119.9, 116.5, 64.4, 25.8, 11.6. HRMS calcd C₃₁H₂₂N₆O₂S₂ 574.1246; found 574.1257.

1-(3-((1-oxo-1-(10H-phenothiazin-10-yl)butan-2-yl)thio)-5H-[1,2,4]triazino[5,6-b]indol-3-yl)hexan-1-one (23). Compound **23** was synthesized similarly to **20**. ¹H NMR (500 MHz, CDCl₃) δ 8.70 (d, *J* = 8.5, 1H), 8.42 (d, *J* = 8.0, 1H), 7.89 (br, 1H), 7.68–7.76 (m, 2H), 7.51–7.60 (m, 2H), 7.40 (br, 1H), 7.27–7.35 (m, 3H), 7.18 (br, 1H), 5.37 (t, *J* = 7.0, 1H), 3.26–3.41 (m, 2H), 2.13 (br, 1H), 1.81–1.90 (m, 3H), 1.28–1.46 (m, 4H), 0.98–1.00 (m, 6H). HRMS calcd for C₃₁H₂₉N₅O₂S₂ 567.1763; found 567.1763.

1-(3-((1-oxo-1-(10H-phenothiazin-10-yl)butan-2-yl)thio)-5H-[1,2,4]triazino[5,6-b]indol-5-yl)pent-4-en-1-one (24). Compound **24** was synthesized similarly to **20**. ¹H NMR (500 MHz, CDCl₃) δ 8.71 (d, *J* = 8.5, 1H), 8.43 (d, *J* = 7.5, 1H), 7.89 (br, 1H), 7.73–7.77 (m, 1H), 7.68 (d, *J* = 6.5, 1H), 7.58–7.61 (m, 1H), 7.51–7.53 (m, 1H), 7.41 (br, 1H), 7.34 (t, *J* = 7.0, 1H), 7.26–7.28 (m, 2H), 7.18 (br, 1H), 5.90–5.98 (m, 1H), 5.36 (t, *J* = 7.0, 1H), 5.10–5.20 (m, 2H), 3.48–3.53 (m, 1H), 3.37–3.43 (m, 1H), 2.57–2.62 (m, 2H), 2.12 (br, 1H), 1.89 (br, 1H), 0.98 (br, 3H). ¹³C NMR (125 MHz, CDCl₃) δ 172.5, 169.9, 167.8, 146.7, 142.4, 139.5, 138.6, 138.3, 136.2, 132.2, 128.3, 127.7, 127.4, 127.3, 126.9, 126.8, 125.9, 121.5, 119.6, 117.8, 116.3, 100.0, 45.8, 38.8, 28.2, 26.1, 11.7. HRMS calcd for C₃₀H₂₅N₅O₂S₂ 551.1450; found 551.1461.

1-(3-((1-oxo-1-(10H-phenothiazin-10-yl)butan-2-yl)thio)-5H-[1,2,4]triazino[5,6-b]indol-5-yl)pent-4-yn-1-one (25). Compound **25** was synthesized similarly to **20**. ¹H NMR (500 MHz, CDCl₃) δ 8.73 (d, *J* = 8.5, 1H), 8.43 (d, *J* = 7.5, 1H), 7.86 (d, *J* = 7.0, 1H), 7.74–7.77 (m, 1H), 7.69 (d, *J* = 7.0, 1H), 7.59–7.62 (m, 1H), 7.54 (d, *J* = 7.5, 1H), 7.34–7.40 (m, 2H), 7.24–7.30 (m, 2H), 7.18 (br, 1H), 5.32 (t, *J* = 7.0, 1H), 3.58–3.62 (m, 1H), 3.45–3.52 (m, 1H), 2.72–2.74 (m, 2H), 2.15 (br, 1H), 1.90 (br, 1H), 1.28 (t, *J* = 7.5, 1H), 0.98–1.01 (m, 3H). HRMS calcd for C₃₀H₂₃N₅O₂S₂ 549.1293; found 549.1294.

5-bromo-1-(3-((1-oxo-1-(10H-phenothiazin-10-yl)butan-2-yl)thio)-5H-[1,2,4]triazino[5,6-b]indol-5-yl)pentan-1-one (26). Compound **26** was synthesized similarly to **20**. ¹H NMR (500 MHz, CDCl₃) δ 8.71 (d, *J* = 8.5, 1H), 8.43 (d, *J* = 7.5, 1H), 7.92 (br, 1H), 7.76 (t, *J* = 8.0, 1H), 7.68 (d, *J* = 7.0, 1H), 7.60 (t, *J* = 7.5, 1H), 7.52–7.54 (m, 1H), 7.41 (br, 1H), 7.30–7.36 (m, 3H), 7.19 (br, 1H), 5.39 (t, *J* = 7.0, 1H), 3.31–3.51 (m, 5H), 2.11 (br, 1H), 1.93–1.98 (m, 2H), 1.85–1.91 (m, 4H), 0.98 (br, 3H). HRMS calcd for C₂₉H₂₄BrN₅O₂S₂ 617.0555; found 617.0543.

Ethyl 5-oxo-5-(3-((1-oxo-1-(10H-phenothiazin-10-yl)butan-2-yl)thio)-5H-[1,2,4]triazino[5,6-b]indol-5-yl)pentanoate (27). Compound **27** was synthesized similarly to **20**. ¹H NMR (500 MHz, CD₃Cl) δ 8.70 (d, *J* = 8.5, 1H), 8.42 (d, *J* = 7.5, 1H), 7.91 (br, 1H), 7.74–7.77 (m, 1H), 7.68 (d, *J* = 7.5, 1H), 7.58–7.61 (m, 1H), 7.52–7.53 (m, 1H), 7.40 (br, 1H), 7.30–7.35 (m, 3H), 7.17 (br, 1H), 5.39 (t, *J* = 6.5, 1H), 3.74 (s, 3H), 3.71–3.72 (m, 2H), 3.42–3.52 (m, 2H), 2.42–2.50 (m, 2H), 1.89–2.02 (m, 2H), 0.98 (br, 3H). ¹³C NMR (125 MHz, CD₃Cl) δ 173.3, 172.5, 169.9, 167.7, 146.6, 142.4, 139.4, 138.6, 138.3, 132.2, 128.3, 127.7, 127.5, 127.3, 127.1, 170.0, 126.8, 125.9, 121.4, 119.6, 117.7, 68.0, 51.8, 38.4, 32.9,

26.0, 19.5, 11.7. HRMS calcd for C₃₁H₂₇N₅O₄S₂ 597.1504; found 597.1498.

General procedure for synthesis of compounds 28–37

Ethyl 2-(3-((1-oxo-1-(10H-phenothiazin-10-yl)butan-2-yl)thio)-5H-[1,2,4]triazino[5,6-b]indol-5-yl)acetate (28). Compound **1** (0.1407 g, 0.3 mmol) was dissolved in 5 ml anhydrous DMF. 50 mg K₂CO₃ and ethyl 2-bromoacetate (0.2004 g, 1.2 mmol) were added to the above solution. This reaction was stirred at room temperature. After 6 h, TLC indicated there was no starting material remained and the reaction was stopped. 150 ml ethyl acetate was added to the above mixture. The organic phase was washed by saturated NH₄Cl for five times and separated. The organic phase was dried by Na₂SO₄ and concentrated. The residue was purified by flash column chromatography (hexane/ethyl acetate-2:1) and viscous oil **28** was obtained. ¹H NMR (500 MHz, CDCl₃) δ 8.39 (d, *J* = 7.5, 1H), 7.88 (br, 1H), 7.62–7.63 (m, 2H), 7.42–7.45 (m, 2H), 7.29–7.32 (m, 2H), 7.19–7.26 (m, 2H), 7.09 (br, 2H), 5.37 (t, *J* = 7.0, 1H), 4.97 (s, 2H), 4.19 (q, *J* = 7.0, 2H), 2.01 (br, 1H), 1.82 (br, 1H), 1.20–1.23 (m, 3H), 0.89–0.91 (m, 3H). HRMS calcd for C₂₉H₂₅N₅O₃S₂ 555.1399; found 555.1405.

2-(3-((1-oxo-1-(10H-phenothiazin-10-yl)butan-2-yl)thio)-5H-[1,2,4]triazino[5,6-b]indol-5-yl)acetic acid (29). Compound **28** (161 mg, 0.2901 mmol) was dissolved in 15 ml 1,4-dioxane and 0.58 ml 1 M NaOH was added to the solution. The reaction mixture was stirred at room temperature. After 14 h, TLC indicated that there was no starting material remained and the reaction was stopped. The pH of the reaction was adjusted to 4–5 using concentrated HAc. The mixture was extracted by ethyl acetate for three times and the organic phase was combined. The organic phase was dried by anhydrous Na₂SO₄ and concentrated under vacuum. The residue was purified by column (DCM/MeOH-60:1) and the viscous oil **29** was obtained. ¹H NMR (500 MHz, CDCl₃) δ 8.42 (d, *J* = 8.0, 1H), 7.94 (br, 1H), 7.62–7.68 (m, 2H), 7.35–7.49 (m, 4H), 7.24–7.30 (m, 3H), 7.07 (br, 1H), 5.40 (t, *J* = 7.0, 1H), 5.01 (s, 2H), 2.03 (br, 1H), 1.84 (br, 1H), 0.92 (br, 3H). HRMS calcd for C₂₇H₂₁N₅O₃S₂ 527.1086; found 527.1093.

2-((5(2-hydroxyethyl)-5H-[1,2,4]triazino[5,6-b]indol-5-yl)thiol)-1-(10H-phenothiazin-10-yl)butan-1-one (30). Compound **28** (95 mg, 0.1712 mmol) was dissolved in 4 ml MeOH/THF (3:1). The solution was cooled to 0°C. Then NaBH₄ (39 mg, 1.027 mmol) was added to the above solution. The reaction mixture was allowed to room temperature. After 6 h, TLC indicated there was no starting material remained and the reaction was stopped. Acetic acid was used to quench the reaction. The mixture was purified by column (hexane/ethyl acetate (5:1-3:1-1:1)) and the viscous oil was obtained. ¹H NMR (500 MHz, CDCl₃) δ 8.44 (d, *J* = 8.0, 1H), 7.99 (br, 1H), 7.72 (t, *J* = 8.0, 1H), 7.66 (br, 1H), 7.59 (d, *J* = 8.0, 1H), 7.47–7.51 (m, 2H), 7.40 (br, 1H), 7.27–7.34 (m, 3H), 7.18 (br, 1H), 5.37 (br, 1H), 4.45 (br, 2H), 4.09 (br, 2H), 2.28 (br, 1H), 2.12 (br, 1H), 1.88 (br, 1H), 0.96 (d, *J* = 7.5, 3H). ¹³C NMR (125 MHz, CDCl₃) δ 170.4, 146.7, 141.6, 138.6, 138.4, 130.9, 127.7, 127.3, 127.2, 126.9, 126.8, 123.1, 122.4, 110.6, 100.0, 60.7, 44.2, 25.9, 11.7. HRMS calcd for C₂₇H₂₃N₅O₂S₂ 513.1293; found 513.1303.

1-(10H-phenothiazin-10-yl)-2-((5(prop-2-yn-1-yl)-5H-[1,2,4]triazino[5,6-b]indol-3-yl)thiol)butan-1-one (31). Compound **31** was synthesized similarly to **28** as amorphous powder. ¹H NMR (500 MHz, CDCl₃) δ 8.48 (d, *J* = 7.5, 1H), 7.59 (br, 1H), 7.75–7.78 (m, 1H), 7.67–7.70 (m, 2H), 7.51–7.55 (m, 2H), 7.40 (br, 1H), 7.31–7.34 (m, 3H), 7.17 (br, 1H), 5.43 (t, *J* = 6.5, 1H), 5.08–5.13 (m, 2H), 2.40 (s, 1H), 1.92 (br, 1H), 1.89 (br, 1H), 0.92–1.01 (m, 3H). HRMS calcd for C₂₈H₂₁N₅O₂S₂ 507.1188; found 507.1188.

2-((5-(but-3-yn-1-yl)-5H-[1,2,4]triazino[5,6-b]indol-3-yl)thio)-1-(10H-phenothiazin-10-yl)butan-1-one (32). Compound **32** was synthesized similarly to **28** as amorphous powder. ¹H NMR (500 MHz, CDCl₃) δ 8.46 (d, *J* = 7.5, 1H), 7.97 (br, 1H), 7.68–7.74 (m, 2H), 7.48–7.59 (m, 3H), 7.40 (br, 1H), 7.31–7.34 (m, 2H), 7.18 (br, 1H), 5.41 (t, *J* = 7.0, 1H), 4.45–4.52 (m, 2H), 2.77–2.80 (m, 2H), 2.14 (br, 1H), 1.89 (br, 1H), 0.98 (br, 3H). ¹³C NMR (125 MHz, CD₃Cl) δ 169.4, 165.9, 145.8, 140.9, 140.6, 137.9, 137.8, 130.9, 128.2, 127.8, 127.5, 127.2, 127.0, 123.0, 121.5, 117.3, 111.6, 80.6, 73.3, 25.7, 17.5, 11.3. HRMS calcd for C₂₈H₂₁N₅O₂S₂ 507.1188; found 507.1188.

2-((5-(2-oxo-2-phenylethyl)-5H-[1,2,4]triazino[5,6-b]indol-3-yl)thio)-1-(10H-phenothiazin-10-yl)butan-1-one (33). Compound **33** was synthesized similarly to **28** as amorphous powder. ¹H NMR (500 MHz, CDCl₃) δ 8.49 (d, *J* = 7.5, 1H), 8.05 (d, *J* = 7.5, 1H), 7.90 (br, 1H), 7.65–7.72 (m, 3H), 7.55–7.58 (m, 2H), 7.49–7.52 (m, 2H), 7.40–7.46 (m, 2H), 7.31–7.39 (m, 1H), 7.21–7.24 (m, 4H), 5.69–5.77 (m, 2H), 5.39 (t, *J* = 6.5, 1H), 2.05 (br, 1H), 1.87 (d, *J* = 5.5, 1H), 0.90–0.92 (m, 3H). HRMS calcd for C₃₃H₂₅N₅O₂S₂ 587.1450; found 507.1461.

2-((5-(1-phenethyl-1H-1,2,3-triazol-4-yl)methyl)-5H-[1,2,4]triazino[5,6-b]indol-3-yl)thio)-1-(10H-phenothiazin-10-yl)butan-1-one (34). 2-bromoethylbenzene (3.083 g, 0.3 mmol) was dissolved in 17 ml anhydrous DMF. NaN₃ (2.1664 g, 33.329 mmol) and 56 mg KI were added to the above solution. The reaction mixture was heated to 90°C for 18 h. TLC indicated that there was no starting material remained. The reaction was stopped and 200 ml DCM was added to the mixture. The organic phase was washed by 50 ml water and dried by anhydrous Na₂SO₄. The organic phase was concentrated and evaporated under vacuum. The crude azide was obtained and used for the next step directly.

Compound **32** (0.1268 g, 0.25 mmol) and azide (33.4 mg, 0.227 mmol) were dissolved in 3.6 ml *t*-BuOH/H₂O/THF (v/v/v:1:1:1). Sodium ascorbate (98.9 mg, 0.4994 mmol) and CuSO₄ (11.3 mg, 0.0454 mmol) in 0.5 ml water were added to the above reaction mixture. The reaction mixture was heated to 55°C. After stirring for 24 h, TLC indicated that there was no starting material remained. The reaction was stopped and cooled to room temperature. 6 ml water was added to the mixture. The solid was collected and washed with a few water. Then, the solid was dissolved in 8 ml acetone and the solution was filtered. The filtrate was evaporated and the residue was dissolved in 3 ml ethyl acetate. The solution was heated and 5 ml hexane was added to the solution. After overnight, gray solid was formed and collected. The amorphous solid **34** was washed by 4 ml hexane and dried. ¹H NMR (500 MHz, CDCl₃) δ 8.44 (d, *J* = 8.0, 1H), 8.03 (br, 1H), 7.66–7.77 (m, 3H), 7.48–7.51 (m, 2H), 7.41 (br, 1H), 7.32–7.33

(m, 2H), 7.18 (br, 1H), 7.06–7.13 (m, 4H), 6.93–6.95 (m, 2H), 5.46–5.56 (m, 3H), 4.53 (t, *J* = 7.5, 2H), 3.14 (t, *J* = 7.5?, 2H), 2.07 (br, 1H), 1.88 (br, 1H), 0.98 (br, 3H). HRMS calcd for C₃₆H₃₀N₈OS₂ 654.1984; found 654.1991.

2-((5-(1-phenethyl-1H-1,2,3-triazol-4-yl)ethyl)-5H-[1,2,4]triazino[5,6-b]indol-3-yl)thio)-1-(10H-phenothiazin-10-yl)butan-1-one (35). Compound **35** was synthesized similarly to **34** as amorphous powder. ¹H NMR (500 MHz, CDCl₃) δ 8.43 (d, *J* = 7.5, 1H), 8.00 (br, 1H), 7.64–7.67 (m, 2H), 7.42–7.50 (m, 4H), 7.23–7.33 (m, 6H), 7.18 (br, 1H), 7.00–7.02 (m, 2H), 6.92 (s, 1H), 5.44 (t, *J* = 6.5, 1H), 4.62 (t, *J* = 7.0, 2H), 4.48 (t, *J* = 7.5, 2H), 3.24 (t, *J* = 7.0, 2H), 3.06 (t, *J* = 7.5, 2H), 2.04–2.08 (m, 1H), 1.87–1.89 (m, 1H), 0.92–1.01 (m, 3H). HRMS calcd for C₃₇H₃₂N₈OS₂ 668.2140; found 668.2135.

Ethyl 4-(2-(3-((1-oxo-1-(10H-phenothiazin-10-yl)butan-2-yl)thio)-5H-[1,2,4]triazino[5,6-b]indol-5-yl)ethyl)-1H-1,2,3-triazol-1-yl)butanoate (36). Compound **36** was synthesized similarly to **34** as amorphous powder. ¹H NMR (500 MHz, CDCl₃) δ 8.41 (d, *J* = 8.0, 1H), 8.01 (br, 1H), 7.62–7.68 (m, 2H), 7.50 (d, *J* = 7.5, 1H), 7.40–7.44 (m, 3H), 7.26–7.33 (m, 3H), 7.17 (br, 2H), 5.44 (t, *J* = 6.5, 1H), 4.66 (t, *J* = 7.0, 2H), 4.32 (t, *J* = 7.0, 2H), 4.15 (q, *J* = 7.0, 2H), 3.29 (t, *J* = 7.0, 2H), 2.20 (t, *J* = 7.5, 2H), 2.07–2.11 (m, 2H), 1.87 (br, 1H), 1.77 (br, 1H), 1.28 (t, *J* = 7.0, 3H), 0.94–1.00 (m, 3H). HRMS calcd for C₃₅H₃₄N₈O₃S₂ 678.2195; found 678.2197.

1-(acridin-10(9H)-yl)-2-((5-(2-hydroxyethyl)-5H-[1,2,4]triazino[5,6-b]indol-3-yl)thio)butan-1-one (37). Compound **37** was synthesized similarly to **30** as viscous oil. ¹H NMR (500 MHz, CDCl₃) δ 8.35 (d, *J* = 7.5, 1H), 7.77 (br, 2H), 7.66–7.70 (m, 1H), 7.55 (d, *J* = 8.0, 1H), 7.44 (t, *J* = 8.0, 1H), 7.24–7.29 (m, 4H), 7.16 (br, 2H), 5.47 (br, 1H), 4.33–4.41 (m, 2H), 4.05–4.08 (m, 2H), 3.86 (br, 2H), 2.13–2.19 (m, 1H), 1.98–1.99 (m, 1H), 1.04 (br, 3H). HRMS calcd for C₂₈H₂₅N₅O₂S 495.1729; found 495.1731.

Acknowledgments

We thank Samy Meroueh for help in initial chemical selection, Sergio C. Chai at St. Jude Children's Research Hospital for help in data analysis of cell growth inhibition, Bert Vogelstein for offering us with cell lines, and all of our colleagues for active discussion and help.

Author Contributions

Conceived and designed the experiments: QZ DRD SZ QZY HL. Performed the experiments: QZ DRD SZ. Analyzed the data: QZ DRD SZ QZY HL. Contributed reagents/materials/analysis tools: QZ DRD SZ QZY HL. Wrote the paper: QZ DRD SZ QZY HL.

References

- Vousden KH, Prives C (2009) Blinded by the Light: The Growing Complexity of p53. *Cell* 137: 413–431.
- Krizhanovsky V, Lowe SW (2009) Stem cells: The promises and perils of p53. *Nature*.
- Hollstein M, Sidransky D, Vogelstein B, Harris CC (1991) p53 mutations in human cancers. *Science* 253: 49–53.
- Brown CJ, Lain S, Verma CS, Fersht AR, Lane DP (2009) Awakening guardian angels: drugging the p53 pathway. *Nat Rev Cancer* 9: 862–873.
- Kruse JP, Gu W (2009) Modes of p53 regulation. *Cell* 137: 609–622.
- Mandinova A, Lee SW (2011) The p53 pathway as a target in cancer therapeutics: obstacles and promise. *Sci Transl Med* 3: 64rv61.
- Vassilev LT, Vu BT, Graves B, Carvajal D, Podlaski F, et al. (2004) In vivo activation of the p53 pathway by small-molecule antagonists of MDM2. *Science* 303: 844–848.
- Issaeva N, Bozko P, Enge M, Protopopova M, Verhoef LG, et al. (2004) Small molecule RITA binds to p53, blocks p53-HDM-2 interaction and activates p53 function in tumors. *Nat Med* 10: 1321–1328.
- Shangary S, Qin D, McEachern D, Liu M, Miller RS, et al. (2008) Temporal activation of p53 by a specific MDM2 inhibitor is selectively toxic to tumors and leads to complete tumor growth inhibition. *Proc Natl Acad Sci U S A* 105: 3933–3938.
- Zhang Q, Zeng SX, Zhang Y, Ding D, Ye Q, et al. (2012) A small molecule Inauhizin inhibits SIRT1 activity and suppresses tumour growth through activation of p53. *EMBO Mol Med* 4: 298–312.
- Zhang Y, Zhang Q, Zeng SX, Mayo LD, Lu H (2012) Inauhizin and Nutlin3 synergistically activate p53 and suppress tumor growth. *Cancer Biol Ther* 13: 915–924.

12. Kgokong JL, Smith PP, Matsabisa GM (2005) 1,2,4-Triazino-[5,6b]indole derivatives: effects of the trifluoromethyl group on in vitro antimalarial activity. *Bioorg Med Chem* 13: 2935–2942.
13. Vang T, Xie Y, Liu WH, Vidovic D, Liu Y, et al. (2011) Inhibition of lymphoid tyrosine phosphatase by benzofuran salicylic acids. *J Med Chem* 54: 562–571.
14. Morin PJ, Sparks AB, Korinek V, Barker N, Clevers H, et al. (1997) Activation of beta-catenin-Tcf signaling in colon cancer by mutations in beta-catenin or APC. *Science* 275: 1787–1790.
15. Dai MS, Lu H (2004) Inhibition of MDM2-mediated p53 ubiquitination and degradation by ribosomal protein L5. *J Biol Chem* 279: 44475–44482.